# The Energy and Solute Conservation Equations for Dendritic Solidification

D.R. POIRIER, P.J. NANDAPURKAR, and S. GANESAN

The energy equation for solidifying dendritic alloys that includes the effects of heat of mixing in both the dendritic solid and the interdendritic liquid is derived. Calculations for Pb-Sn alloys show that this form of the energy equation should be used when the solidification rate is relatively high and/or the thermal gradients in the solidifying alloy are relatively low. Accurate predictions of transport phenomena in solidifying dendritic alloys also depend on the form of the solute conservation equation. Therefore, this conservation equation is derived with particular consideration to an accounting of the diffusion of solute in the dendritic solid. Calculations for Pb-Sn alloy show that the distribution of the volume fraction of interdendritic liquid ($g_L$) in the mushy zone is sensitive to the extent of the diffusion in the solid. Good predictions of $g_L$ are necessary, especially when convection in the mushy zone is calculated.

## I. INTRODUCTION

THE modeling of dendritic solidification has become more sophisticated than the modeling done 10 to 20 years ago in that today the continuity equation, the momentum equation, the energy equation, and the solute conservation equation are simultaneously applied. The most comprehensive exposition of the conservation equations that can be used to model dendritic solidification was given by Hills *et al.*[1] Numerical works include Bennon and Incropera,[2,3,4] Beckermann and Viskanta,[5] Voller and Prakash,[6] Nandapurkar *et al.*,[7] Heinrich *et al.*,[8] and the earliest work of this type done by Szekely and Jassal.[9] In all of the numerical works, the overall concept of solving for temperature, velocity, and solutal concentration has been shared, but there have also been assumptions peculiar to each. In addition, the origins of transport properties, assigned in the two-phase region, have not been consistently exposed.

Several different forms of the momentum equation, as applied to dendritic solidification or closely related scenarios, have been used by various investigators. Recently, Ganesan and Poirier[10] revealed that nonlinear terms in the volume fraction of the liquid phase should be included in the momentum equation. Calculations by Nandapurkar *et al.*[11] showed that the added terms significantly affect thermosolutal convection in both the all-liquid zone and the underlying mushy zone in vertical directional solidification.

The major intent of this article is to present derivations of the energy and solute conservation equations that reveal the origins of appropriate thermodynamic and transport properties for treating mushy zones in dendritic solidification processes, although our derivations and resulting mathematical formulations are not nearly as complete as those of Hills *et al.*[1] A recent contribution pertaining to the conservation equations is that of Rappaz and Voller.[12] However, all of the terms in their momentum equation do not agree with the momentum equation of Ganesan and Poirier,[10] with the exception of the body force term and the pressure gradient term. Similarly, their energy equation and solute conservation equation differ in some respects from the equations that follow in this article. Where it is appropriate, we compare our conservation equations to those of Hills *et al.*[11] for their "metallurgical model."

D.R. POIRIER, Professor, is with the Department of Materials Science and Engineering, The University of Arizona, Tucson, AZ 85721. P.J. NANDAPURKAR, formerly Research Associate, The University of Arizona, is Senior Research Engineer, Dow Chemical, Freeport, TX 77541. S. GANESAN, formerly Graduate Student, The University of Arizona, is Senior Staff Engineer, Motorola, Inc., Phoenix, AZ 85008.

Manuscript submitted July 26, 1990.

## II. THE ENERGY EQUATION

Consider a unit element of constant volume within the mushy zone. With respect to a stationary origin, the unit element is located at $(x, y, z)$. Only the interdendritic liquid convects with velocity $\mathbf{V}(x, y, z, t)$, where $t$ is time and $\mathbf{V}$ is the local average velocity of the interdendritic liquid. The temperatures, $T(x, y, z, t)$, in both solid and liquid, are assumed to be equal. Energy flows into and out of the unit element by conduction, with flux $\mathbf{q}$, and by the advection of the interdendritic liquid, that has a volumetric enthalpy of $Q_L$. Then the energy balance can be written

$$\frac{\partial}{\partial t}(g_s Q_s + g_L Q_L) = -\nabla \cdot \mathbf{q} - \nabla \cdot (g_L Q_L \mathbf{V}) \qquad [1]$$

where $g_s$ and $g_L$ are the volume fractions of solid and liquid, respectively, and $Q_s$ is the volumetric enthalpy of the solid.

Usually, the superficial velocity $\mathbf{U}$ is used, with

$$\mathbf{U} = g_L \mathbf{V} \qquad [2]$$

and the enthalpies are expressed in terms of energy per mass. Therefore,

$$Q_s = \rho_s \bar{H}_s \qquad [3]$$

and

$$Q_L = \rho_L H_L \qquad [4]$$

where $\rho_s$ and $\rho_L$ are the mass densities of the solid and liquid, respectively. The composition of the interdendritic liquid, at a given temperature, is assumed to

be uniform. Consequently, within the unit element, the intensive enthalpy of the interdendritic liquid, $H_L$, is also uniform. Notice, however, that $\bar{H}_s$ is written with an overbar to emphasize that there is microsegregation of solute in the local dendritic solid, so that its intensive enthalpy is an average.

The enthalpies should be expressed with the same thermodynamic reference state, so that at a given temperature,

$$L \equiv H_L - \bar{H}_s \qquad [5]$$

where $L$ is an effective latent heat.

For the conduction flux, we assume that Fourier's law applies and write

$$\mathbf{q} = -\kappa \nabla T \qquad [6]$$

where $\kappa$ is the effective thermal conductivity of the solid plus liquid mixture. This conductivity can be evaluated according to whatever model for two-phase mixtures is thought to be appropriate.[13,14] Notice that the Dufour effect is neglected in Eq. [6], and that the conduction energy flux associated with the overall enthalpy flux can be neglected when it is compared to the advective enthalpy fluxes.

Now by substituting Eqs. [2] through [6] into Eq. [1], the energy equation is written as

$$\frac{\partial}{\partial t}(\bar{\rho}\bar{H}_s + \rho_L g_L L) = \nabla \cdot (\kappa \nabla T) - \rho_L \mathbf{U} \cdot [\nabla(\bar{H}_s + L)] - (\bar{H}_s + L)\nabla \cdot [\rho_L \mathbf{U}] \qquad [7]$$

where $\bar{\rho}$ is the average density of the solid plus liquid mixture, defined as

$$\bar{\rho} = \rho_s g_s + \rho_L g_L \qquad [8]$$

Equation [7] can be simplified somewhat; specifically, if no pores form during solidification, then $dg_s = -dg_L$. Recalling that the solid is assumed not to convect, continuity requires

$$\frac{\partial \bar{\rho}}{\partial t} = -\nabla \cdot (\rho_L \mathbf{U}) \qquad [9]$$

and then by combining Eqs. [7] through [9], the final result is

$$\bar{\rho}\frac{\partial \bar{H}_s}{\partial t} + g_L \rho_L \frac{\partial L}{\partial t} - L\frac{\partial}{\partial t}(g_s \rho_s) = \nabla \cdot (\kappa \nabla T) - \rho_L \mathbf{U}(\nabla \bar{H}_s + \nabla L) \qquad [10]$$

It is preferable to keep the terms with enthalpy as they appear in Eq. [10], because the substitutions

$$\frac{\partial \bar{H}_s}{\partial t} = C_p \frac{\partial T}{\partial t} \qquad [11]$$

and

$$\nabla \bar{H}_s = C_p \nabla T \qquad [12]$$

are not generally valid if the specific heat of the solid, $C_p$, is not carefully considered. Because temperature and composition both change during solidification and the enthalpy of the solid depends on temperature and composition, then $C_p$, as used in Eqs. [11] and [12], is not the thermodynamic heat capacity. By accounting for $\bar{H}_s$ during solidification, it is possible to define $C_p$ so that Eqs. [11] and [12] are applicable, but in so doing, it should be recognized that $C_p$ is not the thermodynamic one. Detailed calculations of the enthalpy of a binary alloy, as it solidifies, were given by Poirier and Nandapurkar.[15]

The latent heat in Eq. [10] is not treated as a constant, and it is carefully defined in Eq. [5] to avoid any ambiguity. It is known that the latent heat varies during solidification of alloys.[15] As an example, during the dendritic solidification of Pb-15 wt pct Sn, the effective latent heat of fusion varies from approximately 51 to 28 $\mathrm{J \cdot g^{-1}}$ from the beginning to the end of solidification,[15,16] whereas the latent heat of lead is 23 $\mathrm{J \cdot g^{-1}}$ at its freezing point.

Equation [10] is similar to the Boussinesq form of the energy equation derived by Hills *et al.*[1] (their Eq. [6.24]) in which they eliminated the Soret effect from their more general result, assumed $\rho_L = \rho_s = \bar{\rho} = \rho$, and took the mixture conductivity, $\kappa$, as uniform. Additionally, if the heat capacity is consistent with Eqs. [11] and [12], then Eq. [10] agrees with Eq. [6.24] in Hills *et al.*[1] Their result includes the possibility of a convecting solid, whereas it is assumed herein that the solid does not convect. For equiaxial dendritic solidification, in which the solid convects, the additional terms introduced by Hills *et al.* and later by Bennon and Incropera[2,4] should be considered. Equation [10] is more explicit, however, in exposing terms with the latent heat of fusion.

The energy equation for the all-liquid zone of a solidifying alloy can be derived from Eq. [10]. This can be seen by reinserting

$$H_L = \bar{H}_s + L$$

from Eq. [5] and simplifying with $g_L = 1$, $g_s = 0$, and $\kappa = \kappa_L$. The result is

$$\frac{\partial H_L}{\partial t} = \frac{1}{\rho_L}\nabla \cdot (\kappa_L \nabla T) - \mathbf{U} \cdot \nabla H_L \qquad [13]$$

Again, substitutions for the terms containing the enthalpy should be carefully made, taking into account that both the composition and the temperature of the liquid in the all-liquid zone can vary.

For the all-solid zone, it is more convenient to start with Eq. [1] and substitute $g_L = 0$ and $g_s = 1$ and Eqs. [3] and [6]. The result is

$$\frac{\partial}{\partial t}(\rho_s \bar{H}_s) = \nabla \cdot (\kappa_s \nabla T) \qquad [14]$$

The solid can comprise more than one constituent (*e.g.*, a primary phase with microsegregation plus an eutectic). Again, before a substitution for $\bar{H}_s$ is made, $C_p$ should be carefully defined.

## III. THE SOLUTE CONSERVATION EQUATION

Solute enters and leaves the unit element (fixed volume) by Fickian diffusion through the liquid and by advection of the interdendritic liquid. Within the unit

element, there can be diffusion in the local solid, but there is no diffusion into or out of the unit element *via* the solid.* For these assumptions, the basic solute balance is

$$\nabla \cdot \mathbf{j} + \nabla \cdot (\rho_L C_L \mathbf{U}) + \frac{\partial}{\partial t}(\overline{\rho C}) = 0 \qquad [15]$$

where $\mathbf{j}$ = Fickian flux of solute, in the interdendritic liquid, $g(\text{solute}) \cdot \text{cm}^{-2} \cdot \text{s}^{-1}$;
$C_L$ = mass fraction of the solute in the interdendritic liquid; and
$\overline{\rho C}$ = mass of the solute per unit volume of the solid plus liquid mixture.

The flux is related to the gradient of the solute mass fraction in the liquid by

$$\mathbf{j} = -\rho_L D_e \nabla C_L \qquad [16]$$

$D_e$ is an effective diffusivity that is defined as

$$D_e = g_L D/\tau \qquad [17]$$

where $D$ is the diffusivity of the solute in the interdendritic liquid and $\tau$ is a tortuosity factor to account for the fact that the boundary of the interdendritic liquid is highly irregular within the dendritic mushy zone. By assuming Fickian diffusion and writing the mass flux as Eq. [16], other contributions to mass flux[1,17] (especially the Soret effect) are neglected.

By combining Eqs. [15] and [16], we get the solute conservation equation in terms of $\overline{C}$:

$$\frac{\partial}{\partial t}(\overline{\rho C}) + \nabla \cdot (\rho_L C_L \mathbf{U}) = \nabla \cdot (\rho_L D_e \nabla C_L) \qquad [18]$$

To make use of Eq. [18], the extent of diffusion in the local solid must be estimated in order to account for the partitioning of the solute between the local dendritic solid and the interdendritic liquid. In turn, this partitioning controls the local value of $g_L$, which directly affects $\mathbf{U}$ and $D_e$ and, consequently, the time derivative of $\overline{\rho C}$ in Eq. [18].

The effect of the extent of diffusion in the solid is examined by considering three cases: (1) complete diffusion, (2) no diffusion, and then (3) some diffusion in the local dendritic solid.

### A. *Complete Diffusion in the Solid*

For this case, the concentration of the solute in the local dendritic solid is uniform, and the transient term in Eq. [18] can be written as

$$\frac{\partial}{\partial t}(\overline{\rho C}) = \frac{\partial}{\partial t}(\rho_s g_s C_s) + \frac{\partial}{\partial t}(\rho_L g_L C_L) \qquad [19]$$

where $C_s$ is the mass fraction of solute in the solid. For a reason to be explained later, both terms on the right-hand side (RHS) of Eq. [19] can be expanded, and Eq. [19] becomes

$$\frac{\partial}{\partial t}(\overline{\rho C}) = \rho_L g_L \frac{\partial C_L}{\partial t} + C_L \frac{\partial}{\partial t}(\rho_L g_L) + k C_L g_s \frac{\partial \rho_s}{\partial t} + k \rho_s C_L \frac{\partial g_s}{\partial t} + k \rho_s g_s \frac{\partial C_L}{\partial t} \qquad [20]$$

For the third, fourth, and fifth terms on the RHS of Eq. [20], $C_L = C_s/k$ has been used; $k$ is the equilibrium partition ratio.

The second term on the left-hand side (LHS) of Eq. [18] is expanded and then combined with Eqs. [8] and [9]. The result of these operations is

$$\nabla \cdot (\rho_L C_L \mathbf{U}) = \rho_L \mathbf{U} \cdot \nabla C_L - C_L g_s \frac{\partial \rho_s}{\partial t} - C_L \rho_s \frac{\partial g_s}{\partial t} - C_L \frac{\partial}{\partial t}(g_L \rho_L) \qquad [21]$$

Finally, Eqs. [18], [20], and [21] are combined to yield the solute conservation equation for the case of complete diffusion in the local solid; it is

$$\left[1 + k\left(\frac{\rho_s g_s}{\rho_L g_L}\right)\right] \frac{\partial C_L}{\partial t} - (1-k) C_L \left(\frac{g_s}{\rho_L g_L}\right) \frac{\partial \rho_s}{\partial t} - \left(\frac{\rho_s C_L}{\rho_L g_L}\right)(1-k) \frac{\partial g_s}{\partial t} + \frac{1}{g_L} \mathbf{U} \cdot \nabla C_L = \left(\frac{1}{\rho_L g_L}\right) \nabla \cdot (\rho_L D_e \nabla C_L) \qquad [22]$$

For many alloys, $\partial \rho_s/\partial t$ can be neglected so Eq. [22] is simplified somewhat, leaving $\partial C_L/\partial t$ as the only transient term to be estimated in a numerical solution.

By defining the average density of the solid plus liquid mixture by Eq. [8], the average mass fraction of the solute in the mixture, $\bar{C}$, is

$$\bar{C} = \frac{\rho_s g_s k C_L + \rho_L g_L C_L}{\rho_s g_s + \rho_L g_L} \qquad [23]$$

Bennon and Incropera[2,3,4] cleverly avoided the formulation in terms of $C_L$ and numerically solved for the new value of $\bar{C}$. Then the local volume fraction of liquid is obtained from Eq. [23]. Because $C_L$ is known by the temperature, Eq. [23] can be used to obtain $g_L$ (with $g_s = 1 - g_L$).

### B. *No Diffusion in the Solid*

For this case, the local solid does not have a uniform concentration of solute. The concentration at the interface is denoted as $C_s^*$ and $\bar{C}_s \neq C_s^*$, where $\bar{C}_s$ is the average mass fraction of solute in the solid. Because there is no diffusion in the solid, then

$$\bar{C}_s = \frac{1}{g_s} \int_0^{g_s} C_s(\eta, t)\, d\eta \qquad [24]$$

where $\eta$ is the coordinate for the local fraction of solid (*i.e.*, $0 \leq \eta \leq g_s$) and values of $C_s$ in the integral are

*Within the unit element itself, the length scale for diffusion in the solid is on the order of tens or hundreds of microns, depending on the local dendrite arm spacings. On the other hand, the length scale for diffusion into or out of the unit element is on the order of ones or tens of centimeters, depending on the average thermal gradient across the mushy zone.

the previous interfacial concentrations that formed when solidification started ($\eta = 0$) to the present fraction of solid ($\eta = g_s$).

By applying Leibnitz's rule to Eq. [24], noting that $\partial C_s/\partial t = 0$ (no diffusion) and $C_s^* = C_s(g_s)$, it can be shown that

$$\frac{\partial}{\partial t}(\rho_s g_s \bar{C}_s) = g_s \bar{C}_s \frac{\partial \rho_s}{\partial t} + \rho_s k C_L \frac{\partial g_s}{\partial t} \qquad [25]$$

Then the time derivative in Eq. [18] can be expanded as follows:

$$\frac{\partial}{\partial t}(\overline{\rho C}) = \rho_L g_L \frac{\partial C_L}{\partial t} + C_L \frac{\partial}{\partial t}(\rho_L g_L) + g_s \bar{C}_s \frac{\partial \rho_s}{\partial t} + \rho_s k C_L \frac{\partial g_s}{\partial t} \qquad [26]$$

Finally, by combining Eqs. [18], [21], and [26], we get the solute conservation equation for no diffusion in the solid. The result is

$$\frac{\partial C_L}{\partial t} - (C_L - \bar{C}_s)\left(\frac{g_s}{\rho_L g_L}\right)\frac{\partial \rho_s}{\partial t} - \left(\frac{\rho_s C_L}{\rho_L g_L}\right)(1-k)\frac{\partial g_s}{\partial t} + \frac{1}{g_L}\mathbf{U}\cdot\nabla C_L = \left(\frac{1}{\rho_L g_L}\right)\nabla\cdot(\rho_L D_e \nabla C_L) \qquad [27]$$

The first term in Eq. [27] differs from the first term in Eq. [22]; all other terms in both equations are exactly the same. The second terms compare by recognizing that $C_s = \bar{C}_s$ when there is complete diffusion in the solid.

In applying Eq. [27], it should be realized that $\bar{C}_s$ is not uniquely related to $C_L$ so that it must be continually evaluated (Eq. [24]). Fortunately, $\partial \rho_s/\partial t$ can be neglected for many alloys; in such cases, the second term is not needed.

Equation [27] reduces to the "local solute redistribution equation," first presented by Flemings and Nereo.[18] Specifically, they assumed that $\rho_s$ is constant, and they did not include diffusion in the liquid (in the direction of the temperature gradient). With these added assumptions, Eq. [27] reduces to

$$\frac{\partial C_L}{\partial t} + \left[\frac{(1-k)C_L}{g_L}\right]\left(\frac{\rho_s}{\rho_L}\right)\frac{\partial g_L}{\partial t} + \left(\frac{1}{g_L}\right)\mathbf{U}\cdot\nabla C_L = 0 \qquad [28]$$

Normally, in dendritic solidification processes, the effect of the diffusion term on solute redistribution is not important. However, thermosolutal convection can play a strong role in the exchange of solute at the transitional region between the mushy zone and the all-liquid zone. Consequently, the very small amount of solute in the vicinity of dendrite tips, in excess of the concentration of the bulk liquid, is critically important in determining the convective stability of the solidifying system.[7] Hence, the inclusion of this term, as in Eq. [27], is recommended for modeling dendritic solidification.

To further check Eq. [27], consider the simplification of $\rho_L = \rho_s =$ constant so that the volume fractions of the phases are the same as the mass fractions ($g_s = f_s$ and $g_L = f_L$). Also, if we ignore both convection and diffusion, then Eq. [27] correctly reduces to the differential form of the well-known Scheil equation,[19] which is often applied as a first approximation to describe microsegregation in dendritic alloys.

On the other hand, solute conservation given by Hills *et al.*[1] (Eq. [6.22] in their article) does not reduce to the Scheil equation but, instead, reduces to the differential form of the "lever rule." Hence, in their solute conservation equation, it is assumed that the concentration of solute in the local solid is uniform and should be comparable to Eq. [22]. Indeed, our Eq. [22] and their Eq. [6.22] are the same when the densities of the two phases are equal and constant, except for the diffusion term.

By substituting Eq. [17] for $D_e$, we get the following term for diffusion:

$$\nabla\cdot\left[g_L\left(\frac{D}{\tau}\right)\nabla C_L\right]$$

whereas the diffusion term (in our notation) from Hills *et al.*[1] results in

$$\frac{D'}{g_L}\nabla\cdot(g_L\nabla C_L)$$

where $D'$ is called the "material diffusion coefficient." By the flux definition given in their Eq. [5.25], it appears that $D' = D/\tau$. However, the two diffusive terms are only equivalent provided $D/\tau$ is spatially uniform and $D/\tau = D'/g_L$. The lack of agreement on this detail between the two models is not apparent. Perhaps, our deduction that $D'$ and $D/\tau$ are equivalent in the two models is in error, or the difference could be explainable with a better descriptive definition of $D'$ by Hills *et al.*

### C. *Some Diffusion in the Solid*

For complete diffusion in the local solid, the time derivative of the amount of solute in the solid is given by the last three terms on the RHS of Eq. [20]. With $kC_L$ replaced by $\bar{C}_s$ (which is valid when there is complete diffusion in the solid), those terms are repeated:

$$\frac{\partial}{\partial t}(\rho_s g_s \bar{C}_s) = g_s \bar{C}_s \frac{\partial \rho_s}{\partial t} + \rho_s k C_L \frac{\partial g_s}{\partial t} + \rho_s g_s k \frac{\partial C_L}{\partial t} \qquad [29]$$

The first term on the RHS exists only if $\rho_s$ is not constant. The second term accounts for the rejection of the solute at the local interface as solidification proceeds by the increment $\partial g_s$. The third term accounts for the diffusion in the solid.

The third term of Eq. [29] does not appear in Eq. [25], which applies for no diffusion in the solid. Thus, by comparing Eqs. [25] and [29], we can write

$$\frac{\partial}{\partial t}(\rho_s g_s \bar{C}_s) = g_s \bar{C}_s \frac{\partial \rho_s}{\partial t} + \rho_s k C_L \frac{\partial g_s}{\partial t} + 2\alpha^* \rho_s g_s k \frac{\partial C_L}{\partial t} \qquad [30]$$

where $\alpha^*$ is the instantaneous diffusion parameter defined by Ganesan and Poirier.[20] For $\alpha^* = 0$, there is

no diffusion, and Eq. [30] reduces to Eq. [25]. For $\alpha^* = 0.5$, there is complete diffusion, and Eq. [30] is the same as Eq. [29]. More generally, $0 \le \alpha^* \le 0.5$, and the third term of the RHS of Eq. [30] accounts for some diffusion in the solid.

Ganesan and Poirier[20] showed that

$$\alpha^* = f(\alpha, k, f_s)$$

where $f_s$ is the weight fraction of solid and $\alpha$ is the Fourier diffusion number, defined as

$$\alpha = D_s t_f / \lambda^2$$

with $D_s$ as the diffusivity in the solid, $t_f$ as the local solidification time, and $\lambda$ as one-half of the characteristic dendrite arm spacing.

Equation [30] leads to a slight modification of Eq. [22] that is obtained after introducing the factor of $2\alpha^*$ and replacing $C_s$ by $\bar{C}_s$. The result is the solute conservation equation for some diffusion in the local solid:

$$\left[1 + 2\alpha^* k\left(\frac{\rho_s g_s}{\rho_L g_L}\right)\right]\frac{\partial C_L}{\partial t} - (C_L - \bar{C}_s)\left(\frac{g_s}{\rho_L g_L}\right)\frac{\partial \rho_s}{\partial t} - \left(\frac{\rho_s C_L}{\rho_L g_L}\right)(1-k)\frac{\partial g_s}{\partial t} + \left(\frac{\mathbf{U}}{g_L}\right)\cdot\nabla C_L = \left(\frac{1}{\rho_L g_L}\right)\nabla\cdot(\rho_L D_e \nabla C_L) \quad [31]$$

Conceptually, Eq. [31] is useful in that it reduces to Eq. [22] and to Eq. [27] with the values of $\alpha^*$ that apply for complete diffusion ($\alpha^* = 0.5$) and no diffusion ($\alpha^* = 0$), respectively. Practically, however, the evaluation of $\alpha^*$ for the case of some diffusion in the solid poses some difficulty to the overall problem of satisfying the momentum and energy equations, as well as the solute conservation equation.

Rather than incorporating the term containing $\alpha^*$ in Eq. [30], it is better to formulate the effect of diffusion in the solid by seeking the solution to Fick's second law for diffusion with appropriate conditions for dendritic solidification. Numerical techniques have been used to make such estimates; previous works include Brody and Flemings,[21] Flemings *et al.*,[22] Nurminen and Brody,[23] Basaran,[24] Kirkwood,[25] Ogilvy and Kirkwood,[26] Battle and Pehlke,[27] and Yeum *et al.*[28] The third term on the RHS of Eq. [30] represents the increase of solute in the solid because of diffusion. This increase of solute in the solid can be obtained by Fick's second law for diffusion and Eq. [24]. First, when Leibnitz's rule is applied, Eq. [30] is replaced with

$$\frac{\partial}{\partial t}(\rho_s g_s \bar{C}_s) = g_s \bar{C}_s \frac{\partial \rho_s}{\partial t} + \rho_s k C_L \frac{\partial g_s}{\partial t} + \rho_s \int_0^{g_s} \frac{\partial C_s}{\partial t} d\eta \quad [32]$$

In order to estimate the integral in Eq. [32] during the period $\Delta t$ from time $t_1$ to time $t_2$, Fick's second law can be used because temperature within the unit element is uniform. Accordingly,

$$\frac{\partial C_s}{\partial t} = \frac{D_s}{\lambda^2}\frac{\partial^2 C_s}{\partial \eta^2} \quad [33]$$

where $\eta$ extends from $\eta = 0$ (the center of the dendrite) to $\eta = g_s$ (the solid/liquid interface), $\lambda$ is a characteristic dimension of the dendrites (*e.g.*, dendrite arm spacing), and $C_s$ is the concentration of solute within the local solid. Also during the period $\Delta t$, $C_s$ must satisfy

$$\frac{\partial C_s}{\partial \eta} = 0 \quad \text{at } \eta = 0 \quad [34]$$

and

$$C_s = C_s^* = kC_L \quad \text{at } \eta = g_s \quad [35]$$

The conditions given by Eqs. [34] and [35] represent no flux at the center of the dendrite and equilibrium at the solid-liquid interface, respectively, and have been invoked in all previous works[20–28] on estimating the extent of diffusion in the solid during solidification of alloys.

In most of the previous estimates of the extent of diffusion in the local solid, one dimensional diffusion and a fixed dendrite arm spacing have been assumed.[21–23,28] The characteristic dimension, $\lambda$, has been adjusted by a factor less than one to compensate for the fact that the dendrites undergo coarsening during solidification.[21–23,28] In the estimates presented by Basaran,[24] Ogilvy and Kirkwood,[25,26] and Battle and Pehlke,[27] the dendrite arm spacing varies during solidification, so in this way, these latter models are more sophisticated than the former. None of the models attempts to treat the complex geometry of the dendrites; therefore, each gives only an estimate of the extent of diffusion in the solid.

During the period $\Delta t$, the local interface advances by the distance $\lambda \Delta g_s$, with $\Delta g_s = g_{s2} - g_{s1}$.* However, $g_{s2}$ is not known and can only be estimated, *e.g.*, by extrapolation from a previous time step. In addition, at time $t_2$, the solute mass balance must be satisfied; *i.e.*,

$$\bar{C}_s f_s + C_L(1 - f_s) = \bar{C} \quad [36]$$

Unfortunately, the problem of solving for diffusion in the solid is a numerical procedure in itself and adds to the overall computational time for obtaining temperature, velocity, and concentrations in a solidifying alloy. To this end, Yeum *et al.*[28] developed an algorithm for estimating diffusion in the solid so that the integral in Eq. [32] can be evaluated efficiently. It should be noted, however, that the algorithm was written for the usual case of solidification with no remelting.

*With convection in the mushy zone, there can be remelting even as the temperature is decreasing because of advection of the solute in the interdendritic liquid. Then $\Delta g_s < 0$.

## IV. SENSITIVITY OF RESULTS TO ASSUMPTIONS

### A. *The Energy Equation*

The energy equation, as represented by Eq. [10], contains four factors that are often neglected or treated inappropriately. They are $\partial L/\partial t$, $\partial \bar{H}_s/\partial t$, $\nabla \bar{H}_s$, and $\partial \rho_s/\partial t$. Here, the intent is to study the sensitivity of some calculated results by isolating the manner in which latent heat and enthalpy are treated for an alloy with a constant $\rho_s$. We solve for the characteristics of the mushy zone

(volume fraction of liquid, height of the mushy zone, and the temperature distribution within the mushy zone) for one-dimensional solidification and examine the sensitivity of these characteristics to the assumptions in the energy equation.

The solidification scenario is shown in Figure 1, which shows a binary alloy undergoing vertical solidification. The mushy zone moves upward with a constant velocity; the isotherms and the isoconcentrates are exactly horizontal. The only convection considered is that within the mushy zone to satisfy continuity ($\rho_s \neq \rho_L$). In an earlier work,[7] a similar problem was solved to define the one-dimensional nonconvecting basic state for a linear stability analysis. For details pertaining to the numerical techniques used herein, we refer the reader to that article.[7]

For the concentration field, we use Eq. [27] with $\partial\rho_S/\partial t = 0$. Then

$$\frac{\partial C_L}{\partial t} + \left[\frac{(1-k)C_L}{g_L}\right]\left[\frac{\rho_S}{\rho_L}\right]\frac{\partial g_L}{\partial t} + \frac{w}{g_L}\frac{\partial C_L}{\partial z} = \frac{1}{\rho_L g_L}\frac{\partial}{\partial z}\left(\rho_L D_e \frac{\partial C_L}{\partial z}\right) \quad [37]$$

where $w$ is the $z$-component of $\mathbf{U}$. As previously mentioned, the interdendritic liquid convects only to satisfy continuity; then, from Eqs. [23] through [25] in Mehrabian *et al.*,[29] it can be shown that

$$\frac{w}{R} = \frac{[g_L(\rho_s - \rho_L) + g_E(\rho_{SE} - \rho_s)]}{\rho_L} \quad [38]$$

where $R$ is the solidification speed, $g_E$ is the volume fraction of eutectic (which forms at the end of solidification), and $\rho_{SE}$ is the density of the eutectic solid.

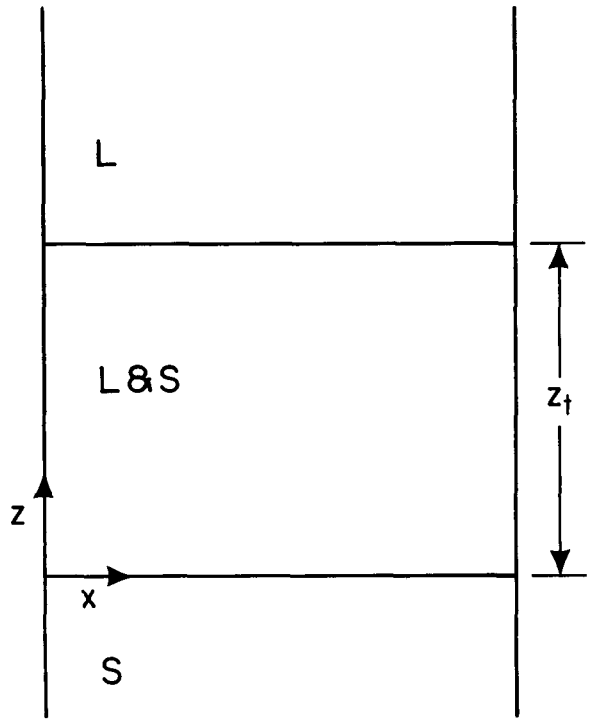


Fig. 1—Geometry and coordinate system for directional solidification of a dendritic alloy.

Because the mushy zone advances with a constant speed $R$, it is convenient to rewrite the energy equation for a coordinate system that moves with the velocity $R$. Then the time derivatives in Eq. [10] are transformed to

$$\frac{\partial \bar{H}_s}{\partial t} = -R\frac{\partial \bar{H}_s}{\partial z} \quad [39]$$

$$\frac{\partial L}{\partial t} = -R\frac{\partial L}{\partial z} \quad [40]$$

and

$$\frac{\partial}{\partial t}(g_s\rho_s) = -R\frac{\partial}{\partial z}(g_s\rho_s) \quad [41]$$

Then, with these substitutions, along with a constant $\rho_s$, Eq. [10] becomes

$$(\rho_L w - \bar{\rho}R)\frac{\partial \bar{H}_s}{\partial z} + (\rho_L w - \rho_L g_L R)\frac{\partial L}{\partial z} - \rho_s L R\frac{\partial g_L}{\partial z} = \frac{\partial}{\partial z}\left(\kappa\frac{\partial T}{\partial z}\right) \quad [42]$$

Without regard for the thermodynamic implications of heats of mixing, Eq. [12] is combined with Eq. [42]; in addition, the latent heat is assumed to be constant so that the energy equation is

$$C_p(\rho_L w - \bar{\rho}R)\frac{\partial T}{\partial z} - \rho_s L R\frac{\partial g_L}{\partial z} = \frac{\partial}{\partial z}\left(\kappa\frac{\partial T}{\partial z}\right) \quad [43]$$

Solidification calculations were done using the thermophysical and transport properties taken from the sources listed in Table I. All of these properties are also summarized in Yeum and Poirier,[16] except the thermal conductivities of the Pb-Sn alloys, which are given in the Appendix.

In the Appendix, the electrical resistivity and thermal conductivity of solid and liquid Pb-Sn alloys from several sources[33–36] are used, in order to obtain sensible extrapolations for estimating the variation of the thermal conductivity of the solid plus liquid mixture during solidification. The results are presented so that

$$\kappa = \kappa(C_L, \bar{C}_s, T, g_s) \quad [44]$$

can be estimated.

Calculations were done to compare the results of applying either Eq. [42] or Eq. [43] to the solidification of

**Table I. Sources for Thermophysical and Transport Properties**

| Property | Reference |
|---|---|
| Densities | |
| $\rho_s$, $\rho_L(C_L)$ | 30 |
| Viscosity | |
| $\mu$ | 31 |
| Enthalpies | |
| $\bar{H}_s(\bar{C}_s, T)$; $H_L(C_L)$ | 15 |
| Phase diagram | |
| $C_L(T)$; $k(T)$ | 32 |
| Diffusivity in liquid | |
| $D = 3 \times 10^{-5}$ cm$^2 \cdot$ s$^{-1}$ | 7 |

Pb-Sn alloys. Specifically, the results of the problem posed by Eqs. [37] and [42] were compared to that posed by Eqs. [37] and [43] under otherwise identical conditions. Solidification rates range from $2 \times 10^{-4}$ cm · s$^{-1}$ to 0.1 cm · s$^{-1}$, compositions include 15, 30, and 50 wt pct Sn, and the temperature gradient in the liquid ($G_L$) at the dendrite tips (where $z = z_t$) is taken as either 30 or 1 K · cm$^{-1}$.

Table II lists computed mushy zone height ($z_t$), volume fraction liquid at the eutectic isotherm ($g_E$), as well as the temperature gradient at the eutectic isotherm, $G_E$, for different solidification rates and concentrations of Sn with $G_L = 30$ K · cm$^{-1}$. For the relatively high value of $G_L$ selected, each characteristic of the mushy zone varies with solidification rate, but each hardly exhibits sensitivity to the choice of the energy equation, except at the highest solidification rate.

Two characteristics of the 30 wt pct Sn alloy, $z_t$ and $G_E$, are plotted in Figure 2, where it can be seen that the computed results are practically insensitive to the choice of the energy equation. At the most, there is a difference of only 6 pct between the predicted values of $z_t$, (Figure 2(a)). The gradient at the eutectic isotherm, $G_E$, is underestimated by a maximum of 12 pct with the simpler energy equation, and that is only for the most rapid solidification rate considered (0.1 cm · s$^{-1}$). Regardless of which energy equation is selected, it is evident that the thermal gradient in the mushy zone is approximately uniform only if $R < 10^{-3}$ cm$^{-1}$.

Computed results, in the form of variation of $g_L$ (volume fraction of interdendritic liquid) and temperature, against the nondimensional position in the mushy zone are shown in Figure 3. Although the most rapid solidification rate has been selected ($R = 0.1$ cm · s$^{-1}$), there is very little difference between the results obtained by either energy equation, because (as explained below) the thermal gradient is rather high.

It was rather surprising to learn that the predictions of the two energy equations are so quantitatively similar, especially because the latent heat of solidification increases from about 23 J · g$^{-1}$ for pure lead (as used in Eq. [43]) to about 51 J · g$^{-1}$ at the end of solidification for 15 wt pct Sn alloy, a difference of more than 100 pct. An order of magnitude analysis reveals that within the mushy zone conduction dominates over the release of latent heat of solidification, and hence, a 100 pct change in the latent heat hardly affects the characteristics of the mushy zone, when $R$ is changed by three orders of magnitude.

For the purpose of the order of magnitude analysis within the mushy zone, Eq. [43] is used. Assuming constant and uniform thermal conductivity and density and further recognizing that $R \gg w$ from Eq. [38], the energy equation simplifies to

$$\kappa \frac{d^2T}{dz^2} + \rho LR \frac{dg_L}{dz} + R\rho C_p \frac{dT}{dz} = 0 \qquad [45]$$

Order of magnitude estimates are as follows:

$$\frac{dT}{dz} \simeq \frac{\Delta T}{z_t}$$

$$\frac{d^2T}{dz^2} \simeq \frac{1}{z_t}\left(\frac{\Delta T}{z_t}\right) \simeq \frac{G_L}{z_t}$$

$$\frac{dg_L}{dz} \simeq \frac{1}{z_t} *$$

*Across the eutectic isotherm, this gradient is discontinuous so that this estimate is not valid. However, on the mushy zone side of this isotherm, this estimate applies.

where

$$\Delta T = T_t - T_E$$

Substituting these estimates into Eq. [45] gives

$$\kappa G_L + (\rho L + \rho C_p \Delta T)R \simeq 0 \qquad [46]$$

For the lead-tin system, typical values of physical parameters are $\kappa \simeq 0.025$, $C_p \simeq 0.1$, $L \simeq 30$, $\Delta T \simeq 100$, and $\rho \simeq 10^4$, all in SI units. Then,

$$0.025G_L + 4 \times 10^5 R \simeq 0 \qquad [47]$$

The first term is the conduction term, and the second is a source term that accounts for the energy released during solidification. With $G_L = 3 \times 10^3$ K · cm$^{-1}$ (a relatively high gradient), the source term is only comparable

**Table II. Sensitivity of Calculated Characteristics of the Mushy Zone to the Energy Equation for Pb-Sn Alloys with $G_L = 30$ K · cm$^{-1}$**

| Case Number | Solidification Conditions | | Computed Results | | | | | |
|---|---|---|---|---|---|---|---|---|
| | | | Eqs. [37] and [43] | | | Eqs. [37] and [42] | | |
| | $R$ (cm · s$^{-1}$) | $C_\infty$ (Wt Pct Sn) | $g_E$ | $G_E$ (K · cm$^{-1}$) | $z_t$ (cm) | $g_E$ | $G_E$ (K · cm$^{-1}$) | $z_t$ (cm) |
| 1 | 0.0002 | 50 | 0.777 | 30.075 | 0.922 | 0.777 | 30.10 | 0.92 |
| 2 | | 30 | 0.386 | 30.178 | 2.470 | 0.389 | 30.20 | 2.467 |
| 3 | | 15 | 0.105 | 30.281 | 3.62 | 0.108 | 30.32 | 3.622 |
| 4 | 0.002 | 50 | 0.784 | 30.609 | 0.916 | 0.785 | 30.70 | 0.91 |
| 5 | | 30 | 0.406 | 31.760 | 2.388 | 0.409 | 32.10 | 2.378 |
| 6 | | 15 | 0.133 | 32.70 | 3.433 | 0.137 | 33.02 | 3.423 |
| 7 | 0.02 | 50 | 0.785 | 30.56 | 0.838 | 0.785 | 30.90 | 0.815 |
| 8 | | 30 | 0.406 | 47.56 | 1.861 | 0.410 | 50.94 | 1.80 |
| 9 | | 15 | 0.135 | 56.96 | 2.305 | 0.140 | 59.65 | 2.268 |
| 10 | 0.1 | 30 | 0.403 | 117.43 | 1.014 | 0.408 | 133.90 | 0.95 |

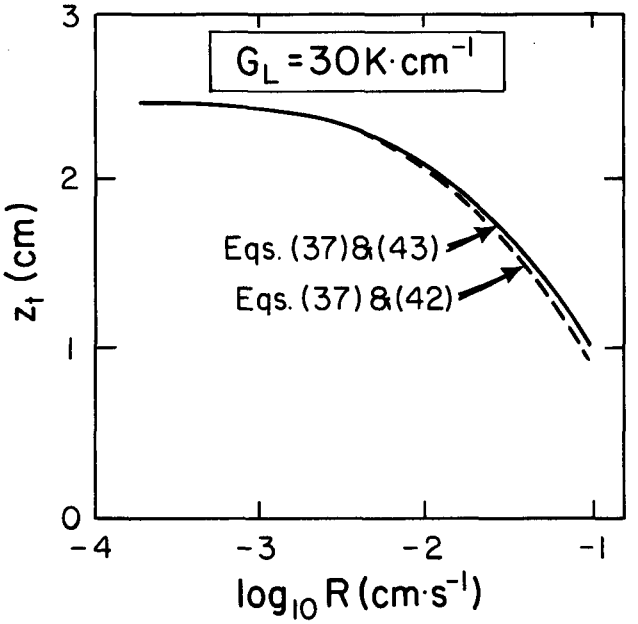


(*a*)

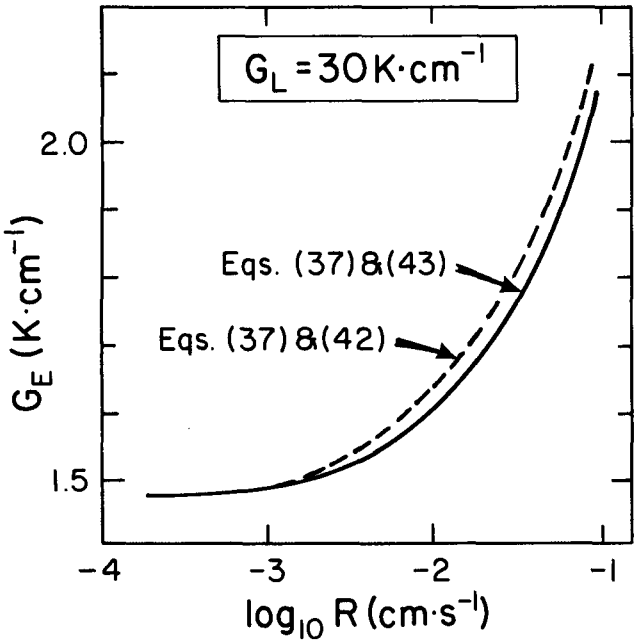


(*b*)

Fig. 2—Effect of the energy equation on 30 wt pct Sn alloy: (*a*) height of the mushy zone, $z_t$, and (*b*) thermal gradient at the eutectic isotherm.

to the conduction term when $R \simeq 0.02$ cm · s$^{-1}$. Therefore, at low solidification rates (*e.g.*, $10^{-4} \leq R \leq 10^{-3}$ cm · s$^{-1}$), the conduction term dominates the source term, and the latent heat of solidification (hence, the choice of the energy equation) does not significantly alter the calculated results with regards to either the mushy zone height or the temperature distribution in the mushy zone. This is also reflected by the numerical computations.

Further, Table II also shows that the value of $g_E$ is almost independent of the energy equation selected. To

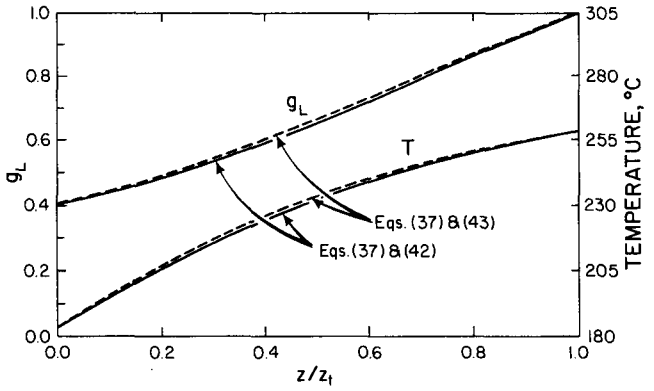


Fig. 3—The volume fraction liquid and temperature calculated for Pb-30 wt pct Sn solidified with $R = 0.1$ cm · s$^{-1}$ and $G_L = 30$ K · cm$^{-1}$.

explain this, the solute conservation equation, Eq. [37], is put into the following form:

$$\left(R - \frac{w}{g_L}\right)\frac{dC_L}{dz} \simeq \frac{(k-1)}{g_L} C_L \frac{dg_L}{dz} \qquad [48]$$

In doing so, the diffusion term in Eq. [37] has been neglected, because $dC_L/dz \simeq$ constant and $D_e$ is small. Thus, $g_L$ is almost uniquely related to $C_L$, and the results are almost independent of the energy equation. The 1 pct difference in $g_E$ is because of the fact that $dC_L/dz$ differs slightly between the two models.

The differences between the two energy equations become more significant when thermal gradients are reduced. To illustrate this, the calculations were repeated for Pb-30 wt pct Sn alloy with $G_L = 1$ K · cm$^{-1}$, which is a realistic thermal gradient for a casting solidifying in a sand mold. The results are given in Table III. Differences between predicted characteristics of the mushy zone for the two models are greater in Table III ($G_L$ = 1 K · cm$^{-1}$) than the differences in Table II ($G_L$ = 30 K · cm$^{-1}$).

It is worthwhile to compare the predicted values of the height of the mushy zone *vs* the heat flux in the solid at the eutectic isotherm. This flux relates to the external cooling of the solidifying metal, because in casting operations, most of the heat is extracted through the solid.

The energy balance at the eutectic isotherm is

$$q_s = \kappa G_E + R g_E [\rho_{SE} L_E + (\rho_{SE} - \rho_{LE}) H_{LE}] \qquad [49]$$

where $q_s$ = heat flux in the solid;
$L_E$ = latent heat of the solidifying eutectic; and
$H_{LE}$ = enthalpy of the eutectic liquid.

Values of $q_s$ were generated using the values of $G_E$, $R$, and $g_E$ in Tables II and III for Pb-30 wt pct Sn. When Eq. [43] was the applicable energy equation, then $L_E$ and $H_{LE}$ were the respective values for pure lead at the eutectic temperature (456 K).

The calculated height of the mushy zone *vs* the heat flux is plotted in Figure 4. With $G_L = 30$ K · cm$^{-1}$, the difference between the values of $z_t$ predicted by the two models is apparent only when $R > 2 \times 10^{-3}$ cm · s$^{-1}$. For example, with a flux of 100 kW · m$^{-2}$, the difference is only 6 pct. However, with $G_L = 1$ K · cm$^{-1}$, the differences are apparent when $R > 2 \times 10^{-4}$ cm · s$^{-1}$, and

**Table III. Sensitivity of Calculated Characteristics of the Mushy Zone to the Energy Equation for Pb-Sn 30 Wt Pct Sn with $G_L = 1\ K \cdot cm^{-1}$**

| Case Number | Solidification Conditions | | Computed Results | | | | | |
|---|---|---|---|---|---|---|---|---|
| | | | Eqs. [37] and [43] | | | Eqs. [37] and [42] | | |
| | $R$ ($cm \cdot s^{-1}$) | $C_\infty$ (Wt Pct Sn) | $g_E$ | $G_E$ ($K \cdot cm^{-1}$) | $z_t$ (cm) | $g_E$ | $G_E$ ($K \cdot cm^{-1}$) | $z_t$ (cm) |
| 11 | 0.0002 | 30 | 0.407 | 1.176 | 67.48 | 0.413 | 1.209 | 66.53 |
| 12 | 0.002 | 30 | 0.405 | 2.747 | 38.76 | 0.408 | 3.087 | 36.70 |
| 13 | 0.02 | 30 | 0.403 | 18.367 | 9.50 | 0.403 | 21.77 | 8.78 |

with a flux of 50 $kW \cdot m^{-2}$, the models differ by approximately 30 pct. Clearly, the more comprehensive form of the energy equation (Eq. [42]) should be used, particularly when the solidification rate is relatively high and/or the thermal gradients are low. The results presented herein are restricted to situations when the cross-couplings of the Dufour and Soret effects are not significant. In the calculations, the temperature gradient in the liquid at the liquidus isotherm has been restricted to $G_L \leq 30\ K \cdot cm^{-1}$ and the solidification speed to $2 \times 10^{-4} \leq R \leq 0.1\ cm \cdot s^{-1}$. These are conditions that typify most dendritic solidification processes. In rapid solidification processes, much steeper thermal gradients and very much faster solidification speeds are encountered, so that cross-coupling effects should be examined.

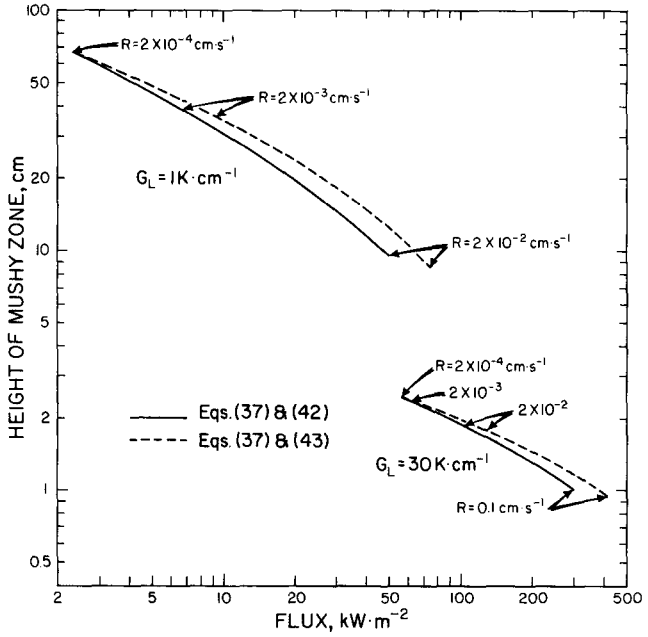


Fig. 4—Calculated height of the mushy zone in Pb-30 wt pct Sn *vs* the heat flux at the eutectic isotherm.

### B. *The Solute Conservation Equation*

Next, the effect of diffusion in the dendritic solid on the characteristics of the mushy zone is considered. Numerical computations, similar to those presented in the previous section, were done, except that complete diffusion in the solid was assumed. Thus, Eq. [22] was used as the solute conservation equation, while the same energy equation, Eq. [42], was kept. In this way, the two extreme situations of no diffusion in the solid (presented in the previous section) and complete diffusion in the solid were compared.

The calculated results are presented in Table IV. For all cases given in Table IV, the effects of diffusion in the solid on the height of the mushy zone ($z_t$) and on the thermal gradient ($G_E$) at the eutectic isotherm are relatively minor or insignificant. The volume fraction of eutectic liquid ($g_E$), however, is substantially reduced by incorporating the effect of diffusion in the solid during solidification of the Pb-30 wt pct Sn alloy. As the concentration of the alloy itself approaches the eutectic concentration (61.9 wt pct Sn), the difference between $g_E$ for no diffusion and $g_E$ for complete diffusion is reduced. This is evident for the calculated values of $g_E$ for the Pb-50 wt pct Sn alloy.

For the case of $R = 2 \times 10^{-3}$ cm $s^{-1}$, $G_L = 30\ K \cdot cm^{-1}$, and an alloy composition of 30 wt pct Sn, calculated results for $g_L$ and temperature are shown in

**Table IV. Sensitivity of Calculated Characteristics of the Mushy Zone to the Extent of Diffusion in the Solid during Solidification for Pb-Sn Alloys with $G_L = 30\ K \cdot cm^{-1}$**

| Case Number | Solidification Conditions | | Computed Results | | | | | |
|---|---|---|---|---|---|---|---|---|
| | | | Eqs. [37] and [42] | | | Eqs. [28] and [42] | | |
| | $R$ ($cm \cdot s^{-1}$) | $C_\infty$ (Wt Pct Sn) | $g_E$ | $G_E$ ($K \cdot cm^{-1}$) | $z_t$ (cm) | $g_E$ | $G_E$ ($K \cdot cm^{-1}$) | $z_t$ (cm) |
| 1 | 0.0002 | 50 | 0.777 | 30.10 | 0.92 | 0.766 | 30.10 | 0.924 |
| 2 | | 30 | 0.389 | 30.20 | 2.467 | 0.286 | 30.23 | 2.467 |
| 4 | 0.002 | 50 | 0.785 | 30.70 | 0.91 | 0.773 | 30.86 | 0.915 |
| 5 | | 30 | 0.409 | 32.10 | 2.378 | 0.317 | 32.27 | 2.378 |
| 7 | 0.02 | 50 | 0.785 | 30.90 | 0.815 | 0.775 | 38.48 | 0.809 |
| 8 | | 30 | 0.410 | 50.94 | 1.80 | 0.316 | 52.6 | 1.78 |
| 10 | 0.1 | 30 | 0.408 | 133.90 | 0.95 | 0.308 | 142.7 | 0.932 |

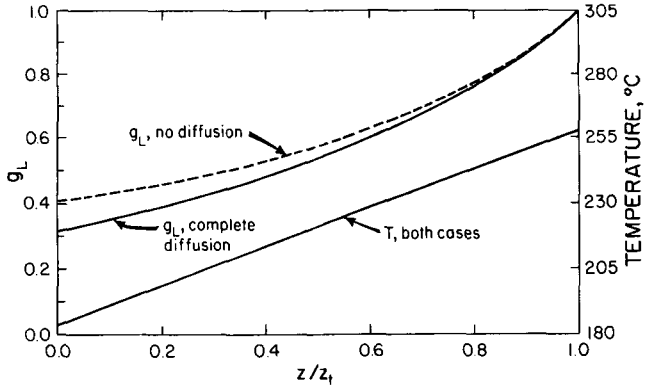


Fig. 5—Effect of diffusion in the solid on the volume fraction liquid and temperature calculated for Pb-30 wt pct Sn solidified with $R = 2 \times 10^{-3}$ cm·s$^{-1}$ and $G_L = 30$ K·cm$^{-1}$.

Figure 5. As mentioned above, the mushy zone height and $G_E$ hardly differ. By far the most important effect of the extent of diffusion in the solid is on the variation of $g_L$ within the mushy zone. With no diffusion in the solid, the mushy zone would also have a greater permeability;[37] thus, if convection within the mushy zone had been considered, it would have been enhanced. In addition, with faster solidification rates and steeper thermal gradients (as in rapid solidification processing), the cross-coupling should be examined.

## V. CONCLUSIONS

Numerical modeling of dendritic solidification is often done to elucidate macrosegregation associated with convection of interdendritic liquid. As mentioned earlier, different conservation equations have been proposed for this purpose in the literature, each with its peculiar set of assumptions. Our aims were to derive the energy equation and the solute conservation equation and to investigate the sensitivity of results to assumptions.

For the simplified problem (one-dimensional mushy zone), we observed the following:

1. With low solidification rates, a rigorous accounting of enthalpy in the energy balance formulation does not significantly affect the height of the mushy zone, the volume fraction of interdendritic liquid, nor the temperature distribution. This insensitivity is caused by the dominant conduction term in the energy equation compared to the heat of solidification term. However, as the solidification velocity increases and/or the thermal gradient decreases, differences between the predicted characteristics of the mushy zone become more pronounced. Although momentum transport was not considered in this work, it is reasonable to suggest that the effects of using the more comprehensive form of the energy equation would be even more apparent, because the advection of the liquid would account for substantially more transport of enthalpy relative to the conduction within the mushy zone. Therefore, it would be more important to properly account for the intensive enthalpies of the liquid and the solid.
2. The effect of diffusion in the dendritic solid is to reduce the volume fraction of interdendritic liquid ($g_L$). This is important when convection of interdendritic liquid is considered, because the permeability of the mushy zone is strongly dependent on $g_L$.

## APPENDIX

### Thermal conductivity of Lead-Tin alloys

*1. Solid Alloys*

The thermal conductivity of the dendritic solid is a function of temperature and the average composition of the solid. As suggested by Turkdogan,[33] the electrical resistivity of a conducting phase comprises an intrinsic resistivity, which depends upon temperature, and a defect resistivity, which depends upon the concentration of defects. It is assumed that the thermal resistivity follows similar behavior; therefore,

$$\delta = \kappa_s^{-1} = \delta_{Pb}(T) + \delta_0(X_{Sn}) \qquad [A1]$$

where $\delta$ is the thermal resistivity, $\kappa_s$ is the thermal conductivity of the solid, $\delta_{Pb}$ is the temperature-dependent thermal resistivity of pure lead (solid), $\delta_0$ is the concentration-dependent part of the thermal resistivity, and $X_{Sn}$ is the atom fraction of Sn.

The thermal conductivity of lead (solid) is given in Touloukian *et al.*[34] from which the following relationship for the thermal resistivity was derived:

$$\delta_{Pb} = \exp [0.01708 \ln T + 0.06294] \qquad [A2]$$

where $T$ = temperature, K; and
$\delta_{Pb}$ = thermal resistivity, cm·K·W$^{-1}$.

The thermal conductivities of both solid lead and solid tin can be represented with linear functions of ln $\kappa$ *vs* ln $T$, with $T$ in kelvins.[34] It is assumed that both solid solutions, the lead-rich phase ($\alpha$) and the tin-rich phase ($\beta$), follow the same behavior. At 327 K, the thermal conductivities of Pb-Sn two-phase alloys[34,35] follow

$$\ln \kappa = f_\alpha \ln \kappa_\alpha + f_\beta \ln \kappa_\beta \qquad [A3]$$

where the subscripts refer to $\alpha$ and $\beta$. Extrapolations of the data for two phases given at 327 K to higher temperatures were based upon the differentiation of Eq. [A3]. Specifically,

$$\left(\frac{\partial \ln \kappa}{\partial \ln T}\right)_C = f_\beta \frac{\partial \ln \kappa_\beta}{\partial \ln T} + f_\alpha \frac{\partial \ln \kappa_\alpha}{\partial \ln T} + \ln \kappa_\beta \frac{\partial f_\beta}{\partial \ln T} + \ln \kappa_\alpha \frac{\partial f_\alpha}{\partial \ln T} \qquad [A4]$$

where

$$\frac{\partial \ln \kappa_\alpha}{\partial \ln T} = \frac{\partial \ln \kappa_{Pb}}{\partial \ln T} = -0.1708$$

and

$$\frac{\partial \ln \kappa_\beta}{\partial \ln T} = \frac{\partial \ln \kappa_{Sn}}{\partial \ln T} = -0.2087$$

The partial derivatives in the third and fourth terms on the RHS of Eq. [A4] were evaluated by an accounting of the relative amounts and the compositions of $\alpha$ and $\beta$ on heating, as computed from the Pb-Sn phase diagram.[32]

The extrapolation procedure yielded a set of thermal conductivities, temperatures, and concentrations for the Pb-rich phase ($\alpha$), from which the concentration-dependent term in Eq. [A1] could be determined. The set of extrapolated values was estimated by a linear polynomial regression; the result is

$$\delta_0 = 1.2581 \times 10^{-3} + 0.18536 X_{Sn}^{1/4} + 6.9496 \times 10^{-2} X_{Sn}^{1/2} \quad [A5]$$

The standard error of fit for $\delta_0$ in Eq. [A4] is $0.0086\ cm \cdot K \cdot W^{-1}$ (less than 8 pct error for all values of $\delta_0$). Together, Eqs. [A1], [A2], and [A5] were used to calculate the thermal conductivity of the Pb-rich phase ($\alpha$), in $W \cdot cm^{-1} \cdot K^{-1}$, as a function of $T$(K) and atom fraction of tin, $X_{Sn}$.

### 2. *Liquid Alloys*

Data for the liquid alloys comprise the thermal conductivities of lead, tin, and Pb-62 wt pct Sn.[34] Based upon the behavior of the electrical conductivity of Pb-Sn melts,[36] it was assumed that

$$\kappa_L = c_0 + c_1 C_{Sn} \quad [A6]$$

where $c_0$ and $c_1$ are temperature-dependent constants and $C_{Sn}$ is in wt pct Sn. Furthermore, it was found that the values of $c_0$ and $c_1$ agreed very closely with the terminal values. Thus,

$$\kappa_L = \kappa_{Pb} + (\kappa_{Sn} - \kappa_{Pb})\,(C_{Sn}/100) \quad [A7]$$

From Touloukian *et al.*,[34] the thermal conductivities of the melts are linear when plotted as $\ln \kappa$ *vs* $\ln T$; thus,

$$\ln \kappa_{Pb} = -6.6777 + 0.7521 \ln T \quad [A8]$$

and

$$\ln \kappa_{Sn} = -3.7518 + 0.4109 \ln T \quad [A9]$$

with $\kappa_{Pb}$ and $\kappa_{Sn}$ in $W \cdot cm^{-1} \cdot K^{-1}$ and $T$ in kelvins. Together, Eqs. [A7] through [A9] are used to calculate the thermal conductivity of the liquid as a function of composition and temperature during solidification.

### 3. *Liquid Plus Solid Alloys*

The thermal conductivity of the mixture of solid and liquid in the mushy zone was assumed to follow a model of two resistors in series, so that

$$\frac{1}{\kappa} = \frac{g_s}{\kappa_s} + \frac{g_L}{\kappa_L} \quad [A10]$$

where $g_s$ and $g_L$ are the volume fractions of solid and liquid, respectively. It is $\kappa$ in Eq. [A10] that was ultimately used as the effective thermal conductivity in the mushy zone.


## ACKNOWLEDGMENTS

The authors are especially grateful for the financial support of the National Aeronautics and Space Administration through Grant No. NAG 3-1060 (Microgravity Sciences and Applications Division). DRP and SG are also grateful for the partial support provided by a contract with the ALCOA Technical Center. We also thank the San Diego Supercomputer Center and Cray Research, Inc., for providing the computational resources on the CRAY Y-MP/864.


## REFERENCES


1. R.N. Hills, D.E. Loper, and P.H. Roberts: *Q. J. Mech. Appl. Math.*, 1983, vol. 36, pp. 505-39.
2. W.D. Bennon and F.P. Incropera: *Int. J. Heat Mass Transfer*, 1987, vol. 30, pp. 2161-70.
3. W.D. Bennon and F.P. Incropera: *Int. J. Heat Mass Transfer*, 1987, vol. 30, pp. 2171-87.
4. W.D. Bennon and F.P. Incropera: *Metall. Trans. B*, 1987, vol. 18B, pp. 611-16.
5. C. Beckermann and R. Viskanta: *Int. J. Heat Mass Transfer*, 1988, vol. 31, pp. 35-46.
6. V.R. Voller and G. Prakash: *Int. J. Heat Mass Transfer*, 1987, vol. 30, pp. 1709-19.
7. P. Nandapurkar, D.R. Poirier, J.C. Heinrich, and S. Felicelli: *Metall. Trans. B*, 1989, vol. 20B, pp. 711-21.
8. J.C. Heinrich, S. Felicelli, P. Nandapurkar, and D.R. Poirier: *Metall. Trans. B*, 1989, vol. 20B, pp. 883-91.
9. J. Szekely and A.S. Jassal: *Metall. Trans. B*, 1978, vol. 9B, pp. 389-98.
10. S. Ganesan and D.R. Poirier: *Metall. Trans. B*, 1990, vol. 21B, pp. 173-81.
11. P.J. Nandapurkar, D.R. Poirier, and J.C. Heinrich: *Numerical Heat Transfer, Part A: Applications*, 1991, vol. 19, pp. 297-311.
12. M. Rappaz and V. Voller: *Metall. Trans. A*, 1990, vol. 21A, pp. 749-53.
13. B. Schulz: in *Thermal Conductivity 18*, T. Ashworth and D.R. Smith, eds., Plenum Press, New York, NY, 1985, pp. 33-43.
14. W.D. Kingery, H.K. Bowen, and D.R. Uhlmann: *Introduction to Ceramics*, 2nd ed., John Wiley and Sons, New York, NY, 1976, pp. 634-37.
15. D.R. Poirier and P. Nandapurkar: *Metall. Trans. A*, 1988, vol. 19A, pp. 3057-61.
16. K.S. Yeum and D.R. Poirier: *Cast Metals*, 1988, vol. 1, pp. 161-70.
17. R.B. Bird, W.E. Stewart, and E.N. Lightfoot: *Transport Phenomena*, John Wiley, New York, NY, 1960, pp. 567-68.
18. M.C. Flemings and G.E. Nereo: *Trans. TMS-AIME*, 1967, vol. 239, pp. 343-47.
19. M.C. Flemings: *Solidification Processing*, McGraw-Hill, New York, NY, 1974, pp. 34-35.
20. S. Ganesan and D.R. Poirier: *J. Cryst. Growth*, 1989, vol. 97, pp. 851-59.
21. H.D. Brody and M.C. Flemings: *Trans. TMS-AIME*, 1966, vol. 236, pp. 615-24.
22. M.C. Flemings, D.R. Poirier, R.V. Barone, and H.D. Brody: *J. Iron Steel Inst.*, 1970, vol. 208, pp. 371-81.
23. J.I. Nurminen and H.D. Brody: in *Titanium Science and Technology*, R.I. Jaffee and H.M. Burte, eds., Plenum Press, New York, NY, 1973, vol. 3, pp. 1893-1914.
24. M. Basaran: *Metall. Trans. A*, 1981, vol. 12A, pp. 1235-43.
25. D.H. Kirkwood: *Mater. Sci. Eng.*, 1984, vol. 65, pp. 101-09.
26. A.J.W. Ogilvy and D.H. Kirkwood: *Appl. Sci. Res.*, 1987, vol. 44, pp. 43-49.
27. T.P. Battle and R.D. Pehlke: *Metall. Trans. B*, 1990, vol. 21B, pp. 357-75.
28. K.S. Yeum, V. Laxmanan, and D.R. Poirier: *Metall. Trans. A*, 1989, vol. 20A, pp. 2847-56.
29. R. Mehrabian, M. Keane, and M.C. Flemings: *Metall. Trans.*, 1970, vol. 1, pp. 1209-20.
30. D.R. Poirier: *Metall. Trans. A*, 1988, vol. 19A, pp. 2349-54.

31. H.R. Thresh and A.F. Crawley: *Metall. Trans.*, 1970, vol. 1, pp. 1531-35.
32. *Metals Handbook*, 8th ed., ASM, Metals Park, OH, 1961, p. 1064.
33. E.T. Turkdogan: *Physical Chemistry of High Temperature Technology*, Academic Press, New York, NY, 1980, p. 124.
34. Y.S. Touloukian, R.W. Powell, C.Y. Ho, and P.G. Klemens: *Thermophysical Properties of Matter, Vol. 1, Thermal Conductivity, Metallic Elements and Alloys*, IFI/Plenum, New York, NY, 1970, pp. 652-54 and 839-41.
35. *Metals Handbook*, 9th ed., ASM, Metals Park, OH, 1979, vol. 2, pp. 505-06.
36. T. Iida and R.I.L. Guthrie: *The Physical Properties of Liquid Metals*, Clarendon Press, Oxford, United Kingdom, 1988, p. 234.
37. D.R. Poirier: *Metall. Trans. B*, 1987, vol. 18B, pp. 245-56.